A Simulation-Based RBDO Method Using Probabilistic Re-Analysis and a Trust-Region Approach

Ramon C. Kuczera
Mechanical Engineering Department
Oakland University, Rochester, MI 48309
Email : ramon.kuczera@gkndriveline.com

Zissimos P. Mourelatos*
Mechanical Engineering Department
Oakland University, Rochester, MI 48309
Phone: 248-370-2686
Fax: 248-370-4416
Email: mourelat@oakland.edu

Efstratios Nikolaidis
Mechanical, Industrial and Manufacturing Engineering Department
The University of Toledo, Toledo, OH 43606
Email: enikolai@eng.utoledo.edu

1st ISSMO Internet Conference on "Reliability-Based Structural Optimization"

***corresponding author**

ABSTRACT

A simulation-based, system reliability-based design optimization (RBDO) method is presented which can handle problems with multiple failure regions. The method uses a Probabilistic Re-Analysis (PRRA) approach in conjunction with a trust-region optimization approach. PRRA calculates very efficiently the system reliability of a design by performing a single Monte Carlo (MC) simulation. Although PRRA is based on MC simulation, it calculates “smooth” sensitivity derivatives, allowing therefore, the use of a gradient-based optimizer. The PRRA method is based on importance sampling. It provides accurate results, if the support (set of all values for which a function is non zero) of the sampling PDF contains the support of the joint PDF of the input random variables and, if the mass of the input joint PDF is not concentrated in a region where the sampling PDF is almost zero. A sequential, trust-region optimization approach satisfies these two requirements. The potential of the proposed method is demonstrated using the design of a vibration absorber, and the system RBDO of an internal combustion engine.

1. INTRODUCTION

In Reliability-Based Design Optimization (RBDO), we often need to estimate repeatedly the reliability of a design for different probability distributions of the input variables. Efficiency and accuracy are therefore, the two main challenges. The reliability, or equivalently the probability of failure, of the system must be calculated accurately and efficiently. The commonly used analytical methods (see section 2) are usually efficient but inaccurate, especially for problems with "noisy" limit states, which may exhibit multiple failure regions and potentially multiple most-probable points (MPPs). Such problems are common in structural dynamics, for example. To alleviate this problem, simulation-based reliability methods may be used. However, they are computationally very expensive and often impractical for many engineering problems.

In probabilistic design, a designer seeks the best configuration to maximize the average utility $U(\mathbf{d}, \mathbf{X}, \mathbf{P})$ of a design. Utility depends on input variables that can be categorized into deterministic design variables $\mathbf{d}$, random design variables $\mathbf{X}$, and random parameters $\mathbf{P}$. Because it is difficult to construct the utility function for a design, alternative formulations are considered. For example, the designer can minimize (or maximize) the average value of an attribute $L(\mathbf{d}, \mathbf{X}, \mathbf{P})$, such as the cost or weight, and impose constraints to satisfy minimum acceptable requirements for the remaining attributes. The system is idealized so that it fails under a finite number of failure modes, and the probability of system failure is calculated from the probabilities of the modes. The probability of system failure is required to be acceptably low.

Let $I(\mathbf{d}, \mathbf{X}, \mathbf{P})$ be the system failure indicator function, which is defined to be one if the system fails and zero if it survives. In system RBDO, the designer seeks the most efficient design whose system probability of failure does not exceed an allowable value p_f^t. The formulation of the system RBDO problem is as follows,

$$\min_{\mathbf{d},\boldsymbol{\mu}_{\mathbf{X}}} E[L(\mathbf{d},\mathbf{X},\mathbf{P})] \tag{1}$$

$$\text{s. t. } p_{sys} = P\,[I(\mathbf{d},\mathbf{X},\mathbf{P}) = 1] \le p_f^t$$

$$\mathbf{d}^L \le \mathbf{d} \le \mathbf{d}^U,\ \text{and}\ \boldsymbol{\mu}_{\mathbf{X}}{}^L \le \boldsymbol{\mu}_{\mathbf{X}} \le \boldsymbol{\mu}_{\mathbf{X}}{}^U.$$

The symbol $E(\cdot)$ indicates the average value operator, and $\mathbf{d}^L$ and $\mathbf{d}^U$, and $\boldsymbol{\mu}_{\mathbf{X}}{}^L$ and $\boldsymbol{\mu}_{\mathbf{X}}{}^U$ are the lower and upper bounds of the deterministic design variables, and the average values of the random design variables, respectively. A bold letter indicates a vector, an upper case letter indicates a random variable or random parameter, and a lower case letter indicates a realization of a random variable or parameter. In subsequent formulations, the bound constraints on the design variables will be omitted. The system probability of failure is defined as $p_{sys} = P\left\{\bigcup_{m=0}^{M}\left(g_m(\mathbf{d},\mathbf{X},\mathbf{P}) \le 0\right)\right\}$ for a series system with M limit states (failure modes).

Probabilistic design problems are often very expensive to solve because the failure probabilities of tens to thousands of alternative designs must be calculated. Moreover, each calculation of the system failure probability requires from few tens to several million deterministic analyses. For a complex structure, such as a car body in crash, each deterministic analysis could require several minutes or hours of CPU time. Studies on reducing the computational cost of probabilistic design have employed the following approaches:

a) Reduce the cost of repeated deterministic analyses by using inexpensive approximations of the attributes which are categorized into global, local or combined approximations [1].

b) Reduce the number of repeated deterministic analyses. For example, if the system failure probability is estimated using MC simulation, many techniques can be used to reduce the number of replications (see simulation-based reliability methods in section 2).

c) Estimate efficiently the moments of the attributes and use them to estimate the probability of failure. Rahman and Xu [2], estimated the moments accurately using one-dimensional integration. Youn *et al*. [3] used this method for efficient estimation of system reliability.

d) Approximate the tail of the cumulative probability distribution of the performance function using a probability distribution that is suitable for representing rare events, such as the Extreme I to III types of distributions and the Generalized Pareto Distribution [4].

This article proposes to circumvent the high computational cost of probabilistic design using a trust-region optimization approach which employs PRRA [5, 6] in each cycle. The approach requires only one MC simulation for each cycle, and estimates the probabilities of failure of tens or hundreds of designs very efficiently using importance sampling. The objectives of this article are 1) to present an overview of the PRRA approach and its strengths, and 2) to integrate PRRA in a trust-region methodology for probabilistic design. The study is confined to design problems where all design variables and parameters are random.

PRRA calculates very efficiently the system reliability for many probability distributions of the input variables, using the results of a single MC simulation for a chosen sampling distribution of the input variables. The method is very efficient because it uses the sample values that are already calculated in a MC simulation, to estimate the reliability for other distributions. In addition, PRRA estimates efficiently the sensitivity derivatives of the reliability with respect to the distribution parameters, which 1) helps identify the important design variables, 2) reduces the cost of optimization, and 3) improves the convergence rate. Furthermore, the reliability estimates and their derivatives vary smoothly (i.e. there is no numerical “noise” due to random sampling), allowing us to use efficient gradient-based optimizers.

After an introduction to the analytical and simulation-based RBDO methods in section 2, we present an overview of the proposed RBDO method in section 3, providing details on the PRRA method in section 3.1, and the proposed "trust-region" RBDO method using PRRA in section 3.2. Section 4 demonstrates the main strengths of PRRA using a vibration absorber example, and section 5 uses the "trust-region" RBDO method on an internal combustion engine example. Finally, summary and conclusions are presented in section 6.

2. ANALYTICAL AND SIMULATION-BASED METHODS IN RBDO

For large-scale systems, the reliability prediction is usually based on efficient computational methods. Both analytical and simulation-based methods are available. The analytical methods are based on the MPP concept. They include the well-known first-order reliability method (FORM) that has been widely used [7], second-order reliability methods (SORM) [8], and multi-point approximation methods [9]. Among the simulation-based methods, the MC simulation method is very simple and accurate. However, its computational cost can be prohibitively high. For this reason, more efficient simulation-based techniques have been proposed [10, 11]. Among them, the adaptive importance sampling (AIS) techniques are popular [12, 13]. A combination of analytical and simulation-based methods has also been used [14]. The analytical methods are generally simple and efficient, but for complex problems, their accuracy cannot be guaranteed. In simulation-based methods, the accuracy can be controlled but the efficiency is generally not satisfactory.

For system reliability analysis involving multiple failure modes (limit states), the joint failure probability must be taken into account. Due to the difficulty in determining the joint failure probability of more than two failure modes except through MC simulation, approximations using first-order and second-order bounds have been developed [15, 16].

Simulation-based methods are also used for reliability analysis involving single or multiple limit states. Among MCS-based methods seeking to improve computational efficiency, adaptive importance sampling (AIS) techniques use an importance sampling density function, which is gradually refined to reflect the increasing state of knowledge of the failure domain. The importance sampling methods are divided into direct methods [11, 17], updating methods [18], spherical schemes [17], directional sampling [19], and adaptive schemes [12, 20]. All methods, except the adaptive schemes, require prior knowledge of the failure domain.

3. OVERVIEW OF PROPOSED RBDO METHOD

It is well known that the analytical reliability methods of section 2 are computationally efficient, and relatively accurate depending on the application. However, their accuracy deteriorates for problems with highly non-linear and/or "noisy" limit states. Also, they are not appropriate for problems with disjoint failure domains and multiple MPPs. Although simulation-based reliability methods can address the shortcomings of the analytical methods, they can be prohibitively expensive for many real-world engineering systems.

In this paper, a simulation-based Probabilistic Re-Analysis (PRRA) method is used in a trust-region, reliability-based design optimization approach. The method uses only three to five MC simulations, to solve system RBDO problems with limit states which can be highly non-linear with multiple MPPs and/or disjoint. In each cycle of the trust-region approach, the PRRA method allows the design to move within a specified domain without additional computational effort, using only a single MC simulation.

Section 3.1 provides an overview of the PRRA method and its capability to provide smooth sensitivities without additional computational effort (section 3.1.1). The smooth sensitivities allow us to use efficient gradient-based optimizers in solving the trust-region sub-optimizations problems. Section 3.2 highlights the main points of the proposed trust-region approach.

3.1. Estimation of Failure Probability in PRRA

The probability of failure of a system is the integral of the joint PDF $f_{\mathbf{X},\mathbf{P}}(\mathbf{x},\mathbf{p})$ of the random design variables **X** and the random parameters **P** over the range of **X** and **P**,

$$p_f = \int_{\mathbf{X},\mathbf{P}} I(\mathbf{x},\mathbf{p})\, f_{\mathbf{X},\mathbf{P}}(\mathbf{x},\mathbf{p})\, d\mathbf{x} \tag{2}$$

where $I(\mathbf{x},\mathbf{p})$ is the failure indicator function.

In Importance Sampling (IS), sample values of the random variables are generated using a sampling PDF $f^S_{\mathbf{X},\mathbf{P}}(\mathbf{x},\mathbf{p})$ that yields many failures with high probability of occurrence, instead of the true PDF $f_{\mathbf{X},\mathbf{P}}(\mathbf{x},\mathbf{p})$. An estimation of the probability of failure in this case is

$$p_f = \int_{\mathbf{X},\mathbf{P}} I(\mathbf{x},\mathbf{p}) \frac{f_{\mathbf{X},\mathbf{P}}(\mathbf{x},\mathbf{p})}{f^S_{\mathbf{X},\mathbf{P}}(\mathbf{x},\mathbf{p})} f^S_{\mathbf{X},\mathbf{P}}(\mathbf{x},\mathbf{p})\, d\mathbf{x}d\mathbf{p}\,, \tag{3}$$

and an unbiased estimator of the probability of failure is provided by,

$$\hat{p}_f = \frac{1}{N}\sum_{i=1}^{N} I(\mathbf{x}_i,\mathbf{p}_i)\frac{f_{\mathbf{X},\mathbf{P}}(\mathbf{x}_i,\mathbf{p}_i)}{f^S_{\mathbf{X},\mathbf{P}}(\mathbf{x}_i,\mathbf{p}_i)} = \frac{1}{N}\sum_{i=1}^{N_f} \frac{f_{\mathbf{X},\mathbf{P}}(\mathbf{x}_i,\mathbf{p}_i)}{f^S_{\mathbf{X},\mathbf{P}}(\mathbf{x}_i,\mathbf{p}_i)} \tag{4}$$

where $\mathbf{x}_i$, $\mathbf{p}_i$, i=1,…, N are the sample values of the random design variables and parameters generated from the sampling PDF $f^S_{\mathbf{X},\mathbf{P}}(\mathbf{x},\mathbf{p})$, and N_f is the number of failures. The sum of the right hand side is only for those replications in which the system fails.

We assume that **X** and **P** are statistically independent, so that $f_{\mathbf{X},\mathbf{P}}(\mathbf{x},\mathbf{p}) = f_{\mathbf{X}}(\mathbf{x}) f_{\mathbf{P}}(\mathbf{p})$, where $f_{\mathbf{X}}(\mathbf{x})$ and $f_{\mathbf{P}}(\mathbf{p})$ are the marginal PDFs. A designer can control the mean value of **X** but not **P.** The key idea of PRRA is that it is sufficient to calculate the failure indicator function of a system only for a single sample of values, $\{\boldsymbol{x}_i , \boldsymbol{p}_i \;\; i = 1,.., N\}$ in order to estimate the system failure probability for other PDFs. Indeed, if one generates a sample from $f^S_{\mathbf{X},\mathbf{P}}(\mathbf{x},\mathbf{p})$ and calculates and saves the sample values that caused system failure $\{\boldsymbol{x}_i , \boldsymbol{p}_i \;\; i = 1,.., N_f\}$, then one can reuse these sample values to estimate the probability of failure $\hat{p}_f$ for another PDF, $f_{\mathbf{X},\mathbf{P}}(\mathbf{x},\mathbf{p})$, as

$$\hat{p}_f = \frac{1}{N}\sum_{i=1}^{N_f} \frac{f_{\mathbf{X}}(\mathbf{x}_i) f_{\mathbf{P}}(\mathbf{p}_i)}{f^S{}_{\mathbf{X},\mathbf{P}}(\mathbf{x}_i, \mathbf{p}_i)}. \tag{5}$$

Eq. (5) holds for any combination of PDFs in the numerator and denominator such that the support (set of all values for which a function is non zero) of $f^S_{\mathbf{X},\mathbf{P}}(\mathbf{x},\mathbf{p})$ contains the support of $f_{\mathbf{X},\mathbf{P}}(\mathbf{x},\mathbf{p})$. This is an important requirement for the accuracy of PRRA.

Eq. (5) allows us to estimate the failure probabilities of many designs very efficiently because it only requires calculation of ratios of PDFs; it does not require calculation of the failure indicator function. This reduces the cost of system reliability analysis by several orders of magnitude because the calculation of the failure indicator function dominates the cost of simulation. The probability of system failure as a function of the mean values of the design variables $\boldsymbol{\mu}_{\mathbf{X}}$ is,

$$\hat{p}_f(\boldsymbol{\mu}_{\mathbf{X}}) = \frac{1}{N}\sum_{i=1}^{N_f} \frac{f_{\mathbf{X}/\boldsymbol{\mu}_{\mathbf{X}}}(\mathbf{x}_i / \boldsymbol{\mu}_{\mathbf{X}}) f_{\mathbf{P}}(\mathbf{p}_i)}{f^S{}_{\mathbf{X},\mathbf{P}}(\mathbf{x}_i, \mathbf{p}_i)} \tag{6}$$

where $f_{\mathbf{X}/\boldsymbol{\mu}_{\mathbf{X}}}(\mathbf{x}/\boldsymbol{\mu}_{\mathbf{X}})$ is the PDF of **X** given the mean value vector $\boldsymbol{\mu}_{\mathbf{X}}$ of the random variables **X**.

An unbiased estimator of the standard deviation of the system failure probability is,

$$\sigma_{\hat{p}_f} = \frac{1}{\sqrt{N(N-1)}} \sqrt{\sum_{i=1}^{N_f} \left(\frac{f_{\mathbf{X},\mathbf{P}}(\mathbf{x}_i, \mathbf{p}_i)}{f^S{}_{\mathbf{X},\mathbf{P}}(\mathbf{x}_i, \mathbf{p}_i)} \right)^2 - N \cdot \hat{p}_f{}^2} \,. \tag{7}$$

Also, the 1-α level confidence interval of the system failure probability is,

$$\hat{p}_f \pm t_{N-1,1-\frac{\alpha}{2}} \cdot \sigma_{\hat{p}_f} \tag{8}$$

where $t_{N-1,1-\frac{\alpha}{2}}$ is the point that has below it probability 1-α/2 for Student's *t*-distribution with (*k*-1) degrees of freedom. This interval covers the true system probability of failure with probability 1-α. Usually, α = 0.05 is used corresponding to the 95% confidence interval.

An algorithm is described below for efficient estimation of the failure probability for many different mean values of the random design variables. This algorithm is used in the trust-region approach of section 3.2.

1. Select a sampling PDF $f^S_{\mathbf{X},\mathbf{P}}(\mathbf{x},\mathbf{p})$ for the random variables.
2. Generate a sample of values for **X** and **P**.
3. Calculate the system failure indicator function, $I(\boldsymbol{x}_i, \boldsymbol{p}_i)$, for the sample values in step 2. Select the subset of sample values that caused system failure.
4. Estimate the system failure probability using Eq. (6). The standard deviation of this probability and a confidence interval can be also calculated using Eqs (7) and (8).

The inputs to PRRA are the sampling PDF, the sample of values that caused failure and the PDF for which the failure probability is to be estimated. The output consists of the probability of failure and its confidence bounds, if needed. PRRA is non-intrusive because it does not require modifications of the computer codes which calculate the values of the limit states.

The estimates of the system failure probability from Eq. (6), and the analytical sensitivities of section 3.1.1, vary smoothly with the design parameters, provided that the sampling and true PDFs are smooth. This is true because the same sample of values of the failure indicator function is used to calculate the failure probability for different values of the design variables. In contrast, the system failure probability varies irregularly when calculated from MC simulation because different samples of random values are used in each simulation. It is not always possible to synchronize a random number generator in MC simulation because each simulation may require a different sample size. An example is the simulation of a system that can fail under different progressive collapse scenarios. In this case, PRRA has an important advantage over MC simulation.

In order to estimate accurately the system failure probability or the average value of a variable, the sample drawn from the sampling PDF should cover adequately the range corresponding to the true PDF. The PRRA method will perform poorly if the mass of the PDF in the numerator of Eq. (6) is concentrated in a region where the sampling PDF is almost zero.

3.1.1 Sensitivity Analysis

It is important to calculate the sensitivity derivatives of the probability of failure with respect to the design variables, and use them in efficient gradient-based optimizers. However, it is impractical to calculate them by a finite difference approach using MC simulation because this requires calculation of the system failure probability of perturbed designs from their nominal values. Each MC simulation can be very expensive and numerical noise in the estimates of the failure probability can amplify the error in the estimates of the sensitivity derivatives.

In PRRA, the sensitivity derivatives of the system failure probability with respect to the RBDO design variables can be calculated analytically by differentiating Eq. (6). For example, the sensitivity derivative with respect to the j^{th} design variable μ_{X_j} is,

$$\frac{\partial \hat{p}_f}{\partial \mu_{X_j}} = \frac{1}{n} \sum_{i=1}^{n_f} \frac{\partial f_{\mathbf{X}/\boldsymbol{\mu}_\mathbf{X})}(\mathbf{x}_i / \boldsymbol{\mu}_X)}{\partial \mu_{X_j}} \frac{f_\mathbf{P}(\mathbf{p}_i)}{f^S{}_{\mathbf{X},\mathbf{P}}(\mathbf{x}_i, \mathbf{p}_i)} \,. \tag{9}$$

In most probabilistic analysis problems, analytical expressions of the random design variable PDFs are available, and these expressions can be differentiated analytically with respect to the average values. The calculation in Eq. (9) is therefore, very efficient because it does not require any additional function evaluations of the limit states.

3.2 Proposed Trust-Region RBDO Method Using PRRA

The trust-region optimization approach uses a number of cycles to locate the final optimum. At each cycle, a sub-optimization problem is solved within a defined sub-domain of the design space using the PRRA algorithm of section 3.1. The sampling PDF $f^S_{\mathbf{X},\mathbf{P}}(\mathbf{x},\mathbf{p})$ at each cycle is chosen such that its variation, measured by the standard deviations of the marginal sampling PDFs, is approximately equal to twice the variation of the actual joint PDF $f_{\mathbf{X},\mathbf{P}}(\mathbf{x},\mathbf{p})$. For normally distributed and statistically independent $\mathbf{X}$ and $\mathbf{P}$, $\boldsymbol{\sigma}^S_\mathbf{X} = 2\boldsymbol{\sigma}_\mathbf{X}$ and $\boldsymbol{\sigma}^S_\mathbf{P} = 2\boldsymbol{\sigma}_\mathbf{P}$. If the distributions are not normal, we can use for example, the difference between the 95th and 5th percentiles as a representative variation measure. For correlated $\mathbf{X}$ and $\mathbf{P}$, we use a normal joint PDF with twice the variation of the actual PDF $f_{\mathbf{X},\mathbf{P}}(\mathbf{x},\mathbf{p})$, where $\boldsymbol{\sigma}^S_\mathbf{X}$, $\boldsymbol{\sigma}^S_\mathbf{P}$ and the correlation coefficient $\rho^S_{\mathbf{X},\mathbf{P}}$ can be estimated using a maximum likelihood estimation (MLE) approach [21, 22], for example. The selection of a normal joint PDF for $f^S_{\mathbf{X},\mathbf{P}}(\mathbf{x},\mathbf{p})$ does not affect the accuracy of the PRRA because we use the actual $f_{\mathbf{X},\mathbf{P}}(\mathbf{x},\mathbf{p})$ to estimate the probability of failure. The sampling PDF can be viewed as an "inflated" actual distribution so that the support of $f^{S}_{\mathbf{X},\mathbf{P}}(\mathbf{x},\mathbf{p})$ contains the support of the true distribution $f_{\mathbf{X},\mathbf{P}}(\mathbf{x},\mathbf{p})$ (see section 2.1). This is an important requirement for the PRRA to provide accurate results.

To demonstrate the steps of the trust-region approach graphically, we use a hypothetical problem with two normally distributed and statistically independent random variables X_1 and X_2 with equal standard deviations, and no random parameters (see Fig. 1). Two limit state functions $g_{1,2} = 0$ are considered. Point **D** represents the deterministic optimum.

The circle centered at point **A** (solid black line denoted by "$\pm 3\boldsymbol{\sigma}^S$ of f^S"), encloses all sample points of $f^{S}_{\mathbf{X},\mathbf{P}}(\mathbf{x},\mathbf{p})$ which are within $\pm 3\boldsymbol{\sigma}^S$, where $\boldsymbol{\sigma}^S$ is the standard deviation vector of the sampling distribution. The other circle centered at point **A** (dotted black line denoted by "$\pm 3\boldsymbol{\sigma}$ of f"), encloses all sample points of $f_{\mathbf{X},\mathbf{P}}(\mathbf{x},\mathbf{p})$ which are within $\pm 3\boldsymbol{\sigma}$, where $\boldsymbol{\sigma}$ is the standard deviation vector of the actual joint distribution. The support of any actual joint distribution "centered" within the "$\pm 3\boldsymbol{\sigma}$ of f" domain will be enclosed by the support of $f^{S}_{\mathbf{X},\mathbf{P}}(\mathbf{x},\mathbf{p})$. This is mathematically represented by $\left\|\boldsymbol{\mu}_{\mathbf{X}} - \boldsymbol{\mu}^{A}_{\mathbf{X}}\right\|_2 \leq 3\boldsymbol{\sigma}$ where $\boldsymbol{\mu}^{A}_{\mathbf{X}}$ and $\boldsymbol{\mu}_{\mathbf{X}}$ denote the mean values of the design variables at point **A**, and at any other location within the "$\pm 3\boldsymbol{\sigma}$ of f" domain, respectively (see Fig. 1).

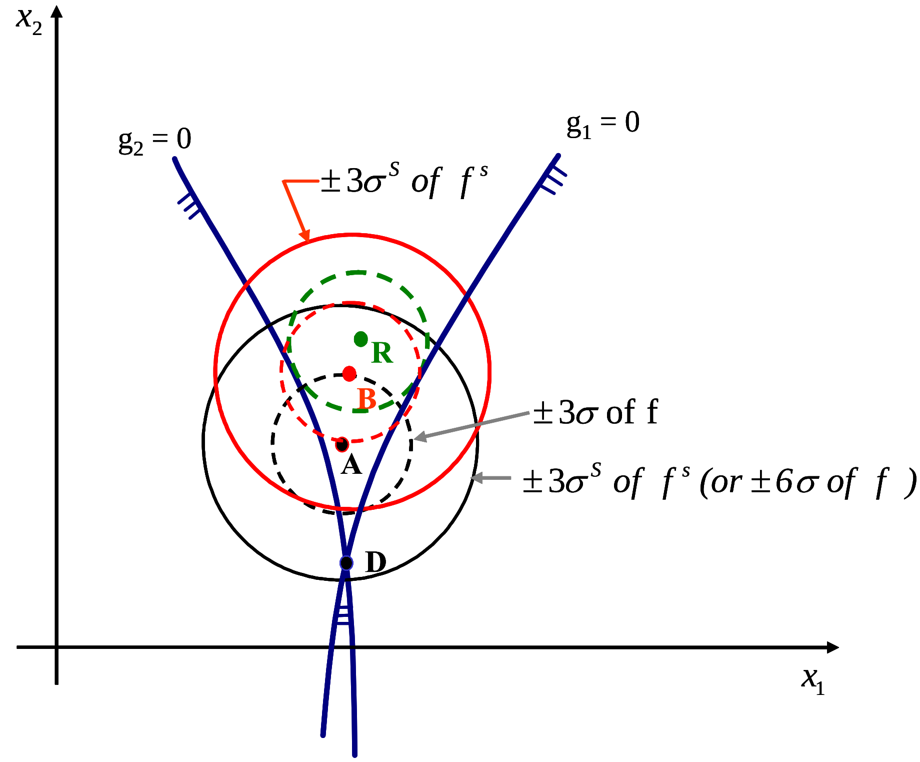

Figure 1. Demonstration of sampling PDF and actual PDFs at different designs.

First, we solve a bi-objective optimization problem in which we minimize a weighted average of the loss function and the failure probability (point **B** represents the optimum design). Then we minimize the loss function while the probability of failure is constrained to be less than an allowable limit (point **R** represents the optimum design).

At the $(k+1)^{th}$ cycle of the trust-region approach, we must solve the following optimization problem,

$$\min_{\mathbf{d}^{k+1},\boldsymbol{\mu}_{\mathbf{X}}^{k+1}} E[L(\mathbf{d}^{k+1},\mathbf{X}^{k+1},\mathbf{P})] \tag{10a}$$

$$\text{s. t.}\quad p_{sys} = P\,[I(\mathbf{d}^{k+1},\mathbf{X}^{k+1},\mathbf{P})=1] \le p_f^t \tag{10b}$$

$$\left\|\boldsymbol{\mu}_{\mathbf{X}}^{k+1}-\boldsymbol{\mu}_{\mathbf{X}}^{k}\right\|_2 \le 3\boldsymbol{\sigma}, \tag{10c}$$

where $\boldsymbol{\mu}_{\mathbf{X}}^{k}$ is the optimum from the k^{th} cycle (e.g. point **A**). The optimization problem of Eq. (10) can be efficiently solved by a gradient-based optimizer using the PRRA algorithm of section 3.1 and the sensitivities of Eq. (9). However, there may not exist a feasible solution. This happens if there is no point in the $\left\|\boldsymbol{\mu}_{\mathbf{X}}^{k+1}-\boldsymbol{\mu}_{\mathbf{X}}^{k}\right\|_2 \leq 3\boldsymbol{\sigma}$ domain which satisfies the $p_{sys}=P\,[I(\mathbf{d}^{k+1},\mathbf{X}^{k+1},\mathbf{P})=1]\leq p_f^t$ constraint. To circumvent this, we solve the following optimization problem, instead of the problem of Eq. (10),

$$\min_{\mathbf{d}^{k+1},\boldsymbol{\mu}_{\mathbf{X}}^{k+1}}\left(E[L(\mathbf{d}^{k+1},\mathbf{X}^{k+1},\mathbf{P})]/E\left[L\left(\mathbf{d}^{k},\mathbf{X}^{k},\mathbf{P}\right)\right]+p_{sys}\right) \tag{11a}$$

$$\text{s. t. } \left\|\boldsymbol{\mu}_{\mathbf{X}}^{k+1}-\boldsymbol{\mu}_{\mathbf{X}}^{k}\right\|_2 \leq 3\boldsymbol{\sigma}\,. \tag{11b}$$

The expected design attribute $E[L(\mathbf{d}^{k+1},\mathbf{X}^{k+1},\mathbf{P})]$ at the current *(k+1)*th cycle is normalized by its value at the k^{th} cycle, and the system probability of failure p_{sys} is added to the normalized value. This represents the solution of the bi-objective optimization problem $\min_{\mathbf{d},\boldsymbol{\mu}_{\mathbf{X}}}\left\{\,E[L(\mathbf{d},\mathbf{X},\mathbf{P})],\quad p_{sys}\right\}$ obtained by the weighted sum method using equal weights for the two objectives.

The optimization problem of Eq. (11) is solved for a few cycles (three to five) until the relative error $\dfrac{\left|f^{k+1}-f^{k}\right|}{\left|f^{k}\right|}$ of the objective, where $f^{k+1}=E[L(\mathbf{d}^{k+1},\mathbf{X}^{k+1},\mathbf{P})]/E\left[L\left(\mathbf{d}^{k},\mathbf{X}^{k},\mathbf{P}\right)\right]+p_{sys}$, is less than 0.5%. The initial point for each cycle is the optimum of the previous cycle. After convergence, the optimization problem of Eq. (10) is solved to get the final optimum. In Fig. 1 for example, the final optimum is represented by point **R**, indicating that both constraints are probabilistically active. The final design is obtained by starting at point **B** which is the optimum of the cycle which started at point **A**.

The internal combustion engine example of section 5 demonstrates the described trust-region approach.

The described trust-region approach requires a MC simulation at each cycle. Although a small number of cycles is required for convergence, and the MC "clouds" overlap between successive cycles allowing us to re-use most of the available sample points, the computational cost may still be high. However, it can be substantially reduced by using radial-based importance sampling techniques [23, 24], "accurate-on-demand" metamodels [25], or a combination of the two. We are currently developing a metamodeling technique which uses importance sampling, a niching genetic algorithm [26, 27], and a lazy learning method for local metamodeling [28, 29]. The technique provides "accuracy-on-demand" based on a user-specified, leave-one-out cross validation mean squared error. Details are provided in [30].

4. A VIBRATION ABSORBER EXAMPLE

4.1 Problem Description

A tuned damper system is shown in Fig. 2. It consists of the original system and a vibration absorber. For simplicity, the original system has a single degree of freedom, and is subject to a harmonic excitation $f(t) = F\cos(\omega \cdot t)$. The absorber is attached to the original system in order to reduce its vibration amplitude. Variations of this problem have been used in the literature [25, 31, 32].

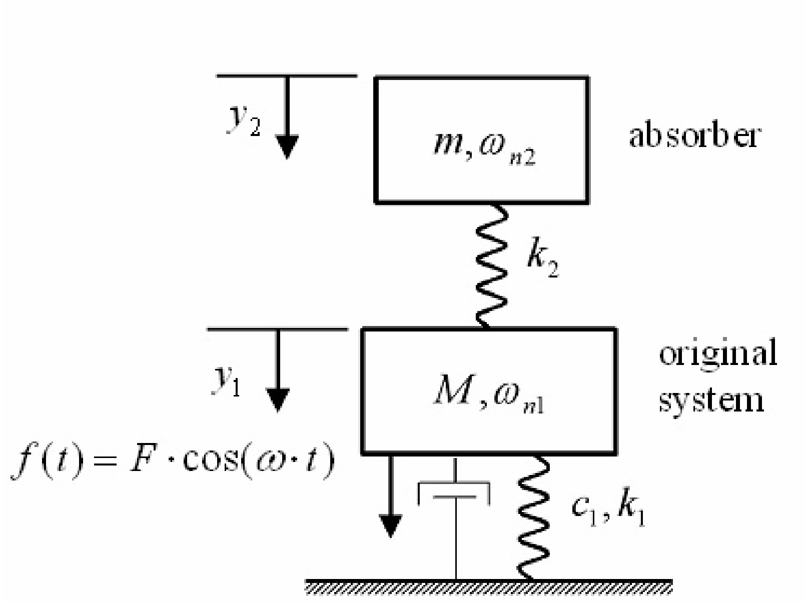

Figure 2. Tuned vibration absorber

The amplitude Y_1 of the original system is a function of four parameters. It is normalized by the amplitude of its static response F / k_1 as follows

$$y_1 = \frac{Y_1}{F/k_1} = \frac{\left|1-(\frac{1}{\beta_2})^2\right|}{\sqrt{\left[1-R(\frac{1}{\beta_1})^2-(\frac{1}{\beta_1})^2-(\frac{1}{\beta_2})^2+\frac{1}{\beta_1^2\beta_2^2}\right]^2+4\varsigma^2\left[(\frac{1}{\beta_1})-\frac{1}{\beta_1\beta_2^2}\right]^2}} \quad (12)$$

In Eq. (12), $R = m/M$ is the ratio of the absorber mass to the original system mass, ς is the damping ratio of the original system, and $\beta_1 = \omega_{n_1}/\omega$ and $\beta_2 = \omega_{n_2}/\omega$ are the ratios of the natural frequencies ω_{n_1} and ω_{n_2} of the original system and vibration absorber respectively, to the excitation frequency ω. It is assumed that the absorber does not provide additional damping to the overall system (see Fig. 2). For illustration, R and ς are treated as deterministic variables with values R=0.01 and ς =0.03, respectively. Only β_1 and β_2 are random variables which are assumed normally distributed with mean 1.0 and standard deviation 0.025.

The absorber is added to “absorb” the vibratory energy when the original system is at resonance or close to resonance. In this case, its motion becomes large, and the motion of the original system reduces considerably. In order for the absorber action to be effective, “tuning” is needed so that the natural frequencies of the absorber and the original system are approximately equal to the excitation frequency ω; i.e. $\omega_{n_1} \approx \omega_{n_2} \approx \omega$, or equivalently, $\beta_1 \approx \beta_2 \approx 1$. With “tuning,” the vibratory amplitude of the original system is almost zero, and the amplitude of the absorber,

$$y_2 = \frac{Y_2}{F/k_1} = \frac{1}{\sqrt{\left[1 - R(\frac{1}{\beta_1})^2 - (\frac{1}{\beta_1})^2 - (\frac{1}{\beta_2})^2 + \frac{1}{\beta_1^2 \beta_2^2}\right]^2 + 4\varsigma^2\left[(\frac{1}{\beta_1}) - \frac{1}{\beta_1 \beta_2^2}\right]^2}} \tag{13}$$

is very high. For durability reasons, the displacement y_2 must be kept below the maximum allowable value of 60.

Fig. 3 shows contours of y_1 and y_2 as a function of β_1 and β_2. There is a trade-off between effective absorber action (small y_1 and simultaneously, large y_2), and absorber durability (small y_2).

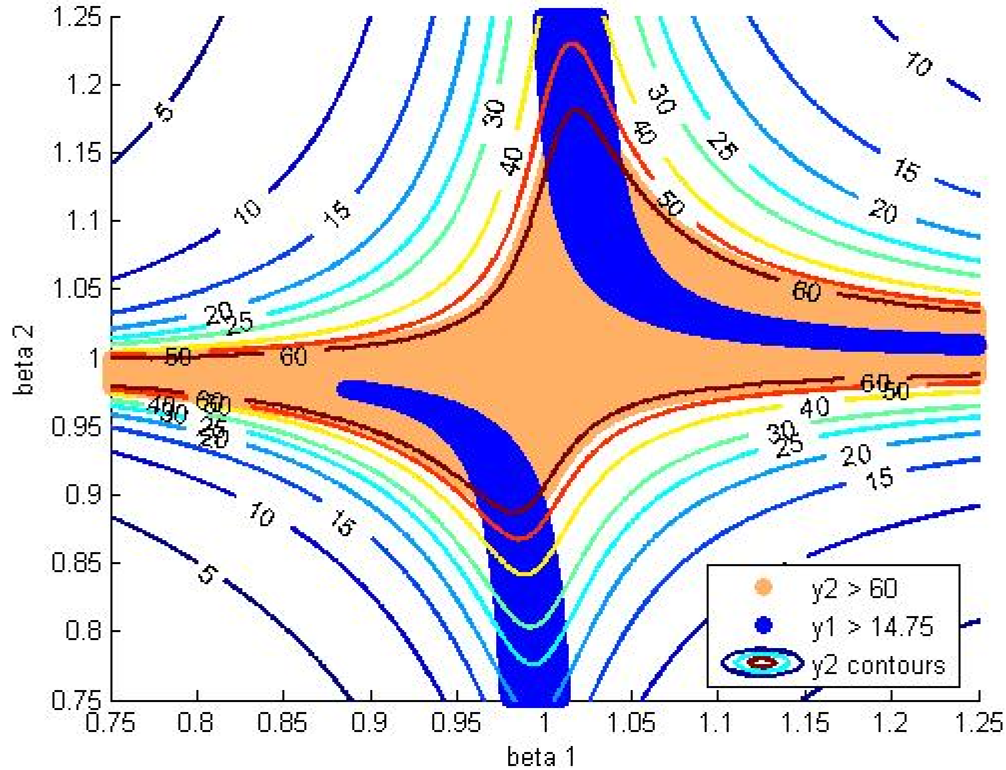

Figure 3. Displacement contours of original system and vibration absorber

The objectives in this example are 1) to maximize the absorber effectiveness by maximizing y_2, and 2) to reduce the risk of the normalized amplitude $y_1(\beta_1, \beta_2)$ exceeding 14.75, if the natural frequencies of the original system and the absorber are uncertain. At the same time, we want $\beta_1 \le 1$ in order to ensure an effective absorber action at "high" excitation frequencies; i.e. $\omega \ge \omega_{n_1}$. To achieve our objectives, the following RBDO problem is solved

$$\max_{\mu_{\beta_1}, \mu_{\beta_2}} y_2\left(\mu_{\beta_1}, \mu_{\beta_2}\right) \tag{14a}$$

$$\text{s.t.} \quad P\left(y_1\left(\beta_1, \beta_2\right) \le 14.75\right) \ge R = 1 - p_f^t, \tag{14b}$$

$$\beta_1 \le 1 \tag{14c}$$

where $\left(\mu_{\beta_1}, \mu_{\beta_2}\right)$ are the means of the two random design variables $\left(\beta_1, \beta_2\right)$, and $R = 1 - p_f^t$ is the target reliability. The target probability of failure is approximated by $p_f^t = \Phi(-\beta^t)$ where β^t is the target reliability index and Φ is the standard normal cumulative distribution function.

In the optimization problem of Eq. (14), we do not use the durability constraint $y_2\left(\beta_1, \beta_2\right) \leq 60$ because it is never active in the presence of constraint (14b).

4.2 Implementation of PRRA

The PRRA method calculates the probability $P\left(y_1\left(\beta_1, \beta_2\right) \leq 14.75\right)$ in the RBDO problem of Eq. (14), using Eq. (6). The sampling PDF is assumed equal to $f^S{}_{\beta_1,\beta_2}(\beta_1, \beta_2) = f^S\left(\beta_1\right) f^S\left(\beta_2\right)$ where $f^S\left(\beta_1\right)$ and $f^S\left(\beta_2\right)$ are normal distributions with mean 1 and standard deviation equal to 0.05 which is twice the actual standard deviation of β_1 and β_2.

The "MCS Hull" in Fig. 4 is a convex hull enclosing all generated sample points from $f^S{}_{\beta_1,\beta_2}(\beta_1, \beta_2)$. The dotted domain denoted by "$\pm 3\sigma$ of f^S," encloses all sample points of the "MCS Hull" which are within $\pm 3\sigma$ of $f^S{}_{\beta_1,\beta_2}(\beta_1, \beta_2)$ where σ is the standard deviation of the sampling distribution. The solid domains denoted by "$\pm 3\sigma$ of f (shifted)," show representative $\pm 3\sigma$ clouds of the actual PDF $f_{\beta_1,\beta_2}(\beta_1, \beta_2)$ for different mean values of β_1 and β_2. The support of $f_{\beta_1,\beta_2}(\beta_1, \beta_2)$, centered at any point within the inner dotted domain, is enclosed by the support of $f^S{}_{\beta_1,\beta_2}(\beta_1, \beta_2)$.

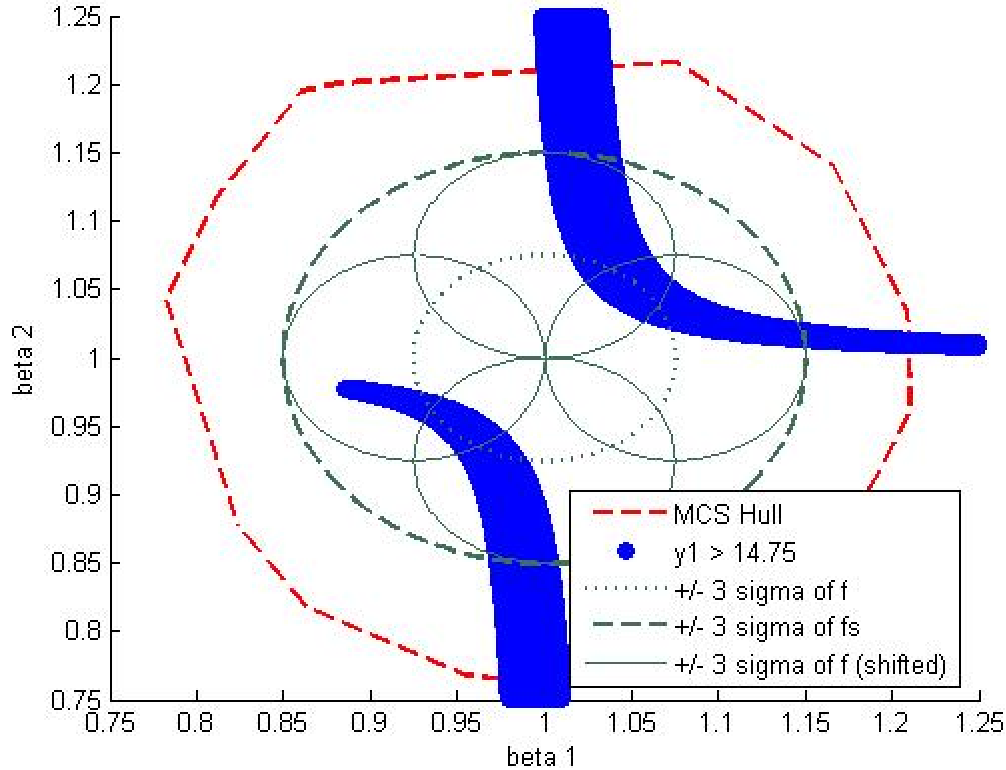

Figure 4. Sampling PDF and actual PDFs at different designs for the vibration absorber

According to the PRRA method, it is sufficient to calculate the value of the failure indicator function for only a single sample of values, $\{ (\beta_{1_i}, \beta_{2_i}),\, i = 1,..,N \}$ of random variables (β_1, β_2) in order to estimate the system failure probability for other PDFs. We therefore, generate a sample from $f^S{}_{\beta_1,\beta_2}(\beta_1, \beta_2)$, calculate the value of the limit state $y_1(\beta_1, \beta_2)$ at each sample point, and save the coordinates of the N_f sample values that caused failure. We then reuse them to estimate the probability of failure $\hat{p}_f$ for another PDF $f_{\beta_1,\beta_2}(\beta_1, \beta_2 / \mu_{\beta_1}, \mu_{\beta_2})$ by reweighing the values of the failure indicator function, as

$$\hat{p}_f(\mu_{\beta_1}, \mu_{\beta_2}) = \frac{1}{N} \sum_{i=1}^{N_f} \frac{f_{\beta_1,\beta_2}(\beta_1, \beta_2 / \mu_{\beta_1}, \mu_{\beta_2})}{f^S_{\beta_1,\beta_2}(\beta_1, \beta_2)} \quad . \tag{15}$$

4.4 Solution of the RBDO Problem

Fig. 5 shows the optimum solution of the RBDO problem of Eq. (14) for different values of the target probability of failure p_f^t, or equivalently the target reliability index β^t. For illustration purposes, the PRRA method was used to identify all points in the inner dotted domain of Fig. 4 which satisfy the probabilistic constraint $P\left(y_1\left(\beta_1, \beta_2\right) \leq 14.75\right) \geq R = 1 - \Phi\left(-\beta^t\right)$ with $\beta^t \geq 3$ (or $p_f \leq 0.00135$). Fig. 5a shows the domain within which $P\left(y_1\left(\beta_1, \beta_2\right) \leq 14.75\right) \geq 1 - \Phi\left(-3\right)$, and Fig. 5b provides a zoomed-in version.

As we maximize y_2, the probabilistic constraint becomes active, resulting in the optimum solution which is indicated by the red points for different values of p_f^t. For p_f^t = 0.00135 ($\beta^t = 3$), the optimum solution is $(\mu_{\beta_1}, \mu_{\beta_2})$ = (0.94828, 1.0405), and for p_f^t = 0.00115, 0.001, and 0.0009, the optimum solution is (0.94635, 1.04211), (0.9463, 1.04356), and (0.94337, 1.04446), respectively. The iso-lines in Fig. 5b indicate the value of y_2.

The values of the calculated probability of failure at the above optimal designs, were validated using a MC simulation with one million sample points. The resulting probabilities of failure are 0.001358, 0.00113, 0.000985, and 0.000927, respectively. All values are very close to the calculated probabilities, indicating that the implementation of the PRRA method in this study provides accurate results.

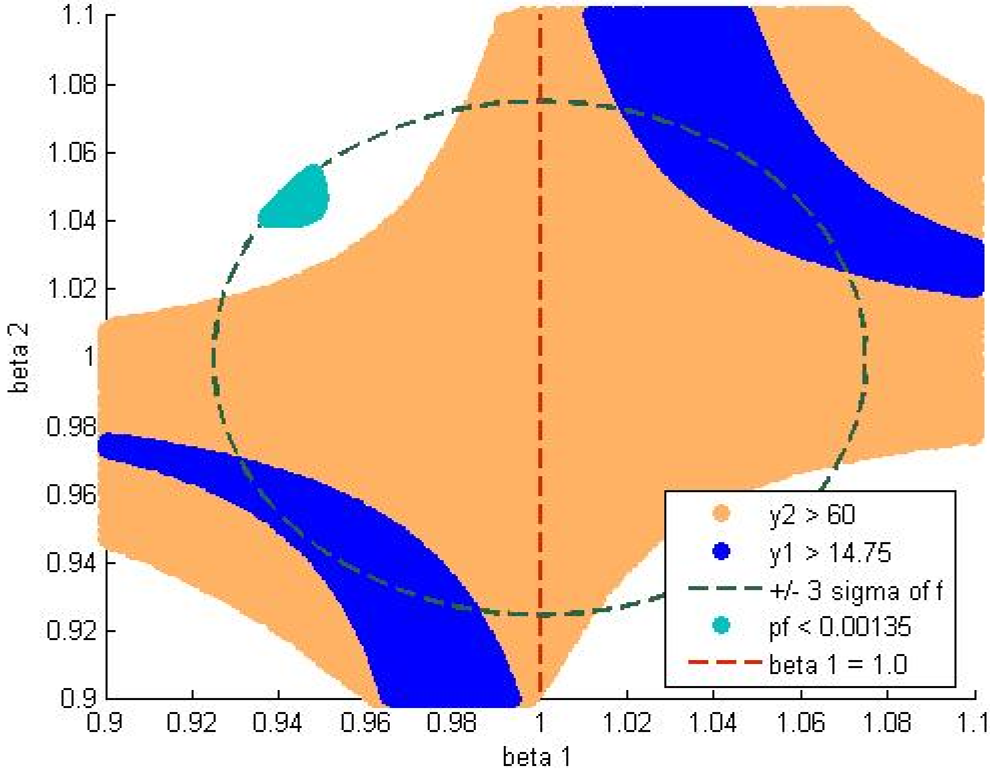

Figure 5a. Optimum solutions for $p_f \leq 0.00135$

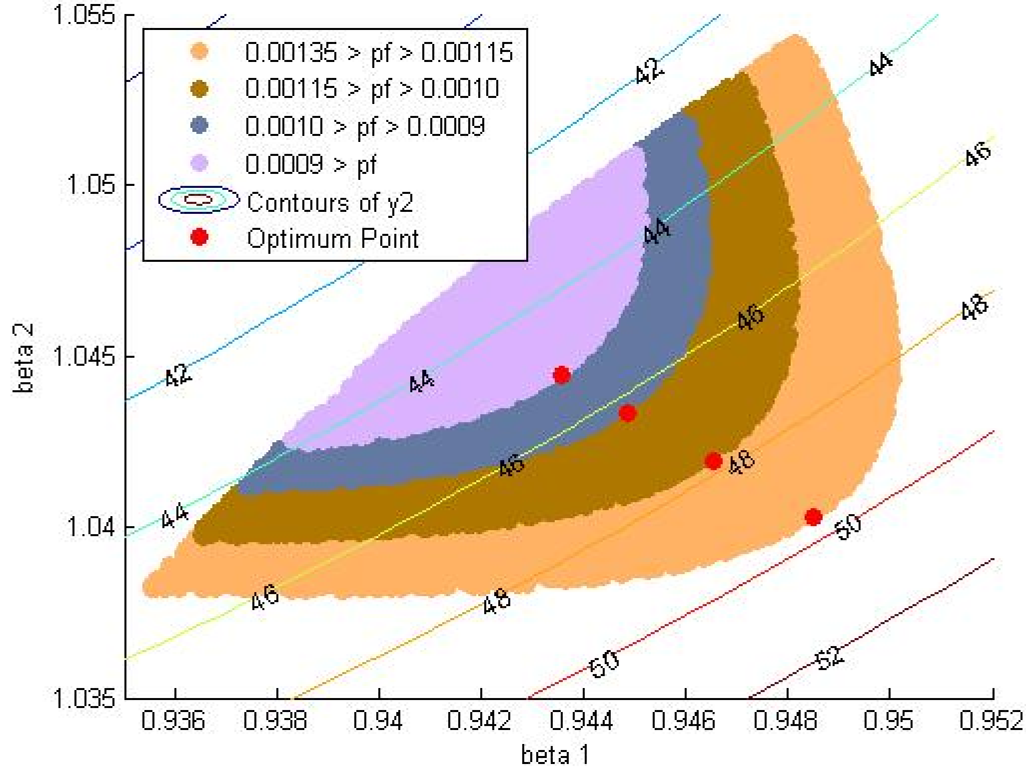

Figure 5b. Optimum solutions for $p_f \leq 0.00135$ (zoomed-in)

5. AN INTERNAL COMBUSTION ENGINE EXAMPLE

This example addresses a flat head design of an internal combustion engine from a thermodynamic viewpoint [33, 34]. Design variables are the cylinder bore b, compression ratio c_r, exhaust valve diameter d_E, intake valve diameter d_I, and the revolutions per minute (RPM) at peak power divided by 1000, ω. The goal is to obtain preliminary values for these variables that maximize the power output per unit displacement while meeting specific fuel economy and packaging constraints. The problem is stated as

Find: $b, d_I, d_E, c_r, \omega, p^t_{f_1}, ..., p^t_{f_9}$

to maximize: $f = \omega[3688\, \eta_t(c_r, b)\eta_v(\omega, d_I) - FMEP\ (c_r, \omega, b)]/120$

where,

$$FMEP = 4.826(c_r - 9.2) + 7.97 + 0.253 \cdot [8V / (\pi N_c)] \cdot \omega b^{(-2)} + 9.7 \cdot 10^{-6}\{[8V/(\pi N_c)] \cdot \omega b^{(-2)}\}^2,$$

$$\eta_t = 0.8595(1 - c_r^{-0.33}) - S_v(1.5/\omega)^{0.5},$$

$$S_v = 0.83 \cdot [8 + 4c_r + 1.5(c_r - 1)b^3 \pi N_c / V]/[(2 + c_r) \cdot b],$$

$$\eta_v = \eta_{vb}(1 + 5.96 \cdot 10^{-3}\omega^2)/\{1 + [9.428 \cdot 10^{-5} 4V/(\pi N_c C_s)(\omega / d_I^2)]^2\}$$

$$\eta_{vb} = \begin{cases} 1.067 - 0.038\ e^{(\omega - 5.25)}\ for\quad \omega \ge 5.25 \\ 0.637 + 0.13\,\omega - 0.014\,\omega^2 + 0.00066\,\omega^3\ for\quad \omega \le 5.25 \end{cases},$$

subject to:

$$p_{sys} \le p^t_f$$

where $p_{sys} = P(\bigcup_{i=1}^{9} G_i(\mathbf{X}) \le 0)$ is the system failure probability and $p^t_f = 0.006539$ is the target probability of failure for the system. The nine constraints are listed below:

$G_1 = 400 - 1.2N_c b$ (min. bore wall thickness),

$G_2 = b - [8V/(200\pi N_c)]^{0.5}$ (max. engine height),

$G_3 = 0.82b - d_I - d_E$ (valve geometry & structure),

$G_4 = d_E - 0.83d_I$ (min. valve diameter ratio),

$G_5 = 0.89d_I - d_E$ (max. valve diameter ratio),

$G_6 = 0.6C_s - 9.428 \cdot 10^{-5}(4V/\pi N_c)(\omega / d_I^2)$ (max. Mech Index),

$G_7 = 0.045 \cdot b - c_r + 13.2$ (knock-limit compression ratio),

$G_8 = 6.5 - \omega$ (max. torque converter RPM),

$G_9 = 230.5 Q \eta_{tw} - 3.6 \cdot 10^6$ (max. fuel economy),

with $\eta_{tw} = 0.8595 \cdot (1 - c_r^{-0.33}) - S_V$, $V = 1.859 \cdot 10^6 (mm^3)$, $Q = 43{,}958 kJ / kg$, $C_S = 0.44$, and $N_c = 4$. Many of the above expressions are valid only within the limited range of bore-to-stroke ratio of $0.7 \le b/s \le 1.3$. More information on the problem definition can be found in [33]. All design variables are assumed normal with standard deviation and bounds as shown in Table 1.

Table 1. Distribution parameters and bounds of design variables

	Standard Deviation	**Lower Bound**	**Upper Bound**
cylinder bore, b, mm	0.4	70	90
intake valve diameter, d_I, mm	0.15	25	50
exhaust valve diameter, d_E, mm	0.15	25	50
compression ratio, c_r	0.05	6	12
RPM at peak power/1000, ω	0.25	5	12

Liang *et al*. [35] solved this system RBDO problem by using a first-order reliability method (FORM) to calculate the probability of violating each of the nine constraints above and the upper, second-order Ditlevsen bound [16] to calculate the system failure probability. The allowable system failure probability was 0.006539 (same as in this study). They also solved the corresponding component RBDO problem by constraining the probabilities of violating each constraint to be less than or equal to a maximum allowable value of 0.00135. For comparison purposes, Table 2 presents the solutions of the component and system RBDO problems in [35].

Table 2. Comparison of results for internal combustion engine example (Liang *et al*. [35])

Design Variables	**Deterministic Optimization**	**Component**	**System**
b	83.3333	82.1333	82.1419
d_I	37.3406	35.8430	35.8456
d_E	30.9927	30.3345	30.3641
c_r	9.4500	9.3446	9.3174
ω	6.0720	5.3141	5.3598
p_{f_1}		0.00135	0.001448
p_{f_3}		0.00135	0.001665
p_{f_4}		0.00135	0.000811
p_{f_6}		0.00135	0.002370
p_{f_7}		0.00135	0.000232
p_{sys}		0.00675	0.006539
Objective f(X)	55.6677	50.9713	51.1023

The sensitivity derivative of the system failure probability to the bore is calculated using Eq. (9) and is shown in Fig. 6. It is observed that the derivative of the system failure probability is negative for bore values less than 82.1 mm, zero for 82.1 mm, and positive for greater values. This means that the probability of failure is minimized at 82.1 mm. These observations are consistent with the results from this study (see optimum value of bore in last column of Table 3).

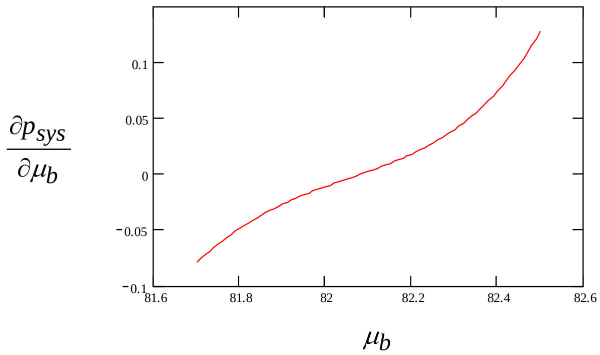

Figure 6. Sensitivity Derivative of System Failure Probability

Table 3. Comparison of results for internal combustion engine example (present study)

		Initial Design	**Cycle # 1**	**Cycle # 2**	**Cycle # 3**	**Cycle # 4**	**Final Design**
Design Variables	b	83.3333	82.9146	82.6377	82.2857	82.2818	82.1537
	d_I	35.9744	36.8906	36.4406	35.9906	35.9829	35.846
	d_E	30.4287	30.841	30.6644	30.4281	30.4348	30.3777
	c_r	9.5042	9.4106	9.4638	9.6138	9.6482	9.7982
	ω	5.4734	5.8377	5.6167	5.4819	5.484	5.378
Probabilities of Failure	p_{f1}	0.4997	0.1476	0.0410	0.0043	0.0044	0.0016
	p_{f2}	0	0	0	0	0	0
	p_{f3}	0	0.2547	0.0460	0.0034	0.0035	0.0017
	p_{f4}	0.0018	0.1268	0.0161	0.0022	0.0017	0.0007
	p_{f5}	0	0	0	0	0	0
	p_{f6}	0.0054	0.0091	0.0045	0.0057	0.0059	0.0030
	p_{f7}	0	0	0	0	0	0
	p_{f8}	0	0.0040	0.0002	0	0	0
	p_{f9}	0	0	0	0	0	0
	p_f^{sys} **(MC)**	0.5033	0.4867	0.1060	0.0155	0.0154	0.0067
	p_f^{sys} **(PRRA)**	0.4957	0.4651	0.1082	0.0145	0.0152	0.0065
	Objective	**55.6677**	**54.4956**	**53.2927**	**52.3576**	**52.4155**	**52.0682**

We used the deterministic optimum as initial point in the trust-region approach (see Table 3). Only 100,000 sample points were used in the MC simulation of each cycle. We found that 100,000 sample points provided good accuracy in this example. The trust-region approach needed four cycles to converge. The relative error of the objective after the 4th cycle is 0.11% ((52.4155 - 52.3576)*100/52.3576). At this point, the optimization problem of Eq. (10) was solved to obtain the final optimum of the last column in Table 3. The 52.0682 optimum is better than the 51.1023 optimum in [35] because the present study does not use FORM approximations.

The second from last row lists the system probability of failure as calculated by PRRA. As expected, the deterministic design has a very high probability of 0.4957 because it is on boundary of the feasible domain. The probability of failure drops very quickly to 0.0152 after the 4th cycle, indicating a fast convergence of the trust-region approach. At the end of each cycle and at the initial and final designs, we verified the accuracy of our results with MC simulation with one million sample points. The 3rd from last row shows the MC-based p_{sys} which is very close to the PRRA-based p_{sys}.

At the optimum, the component probabilities of failure (p_{f_1} to p_{f_9} in Table 3) indicate that only the 1st, 3rd, 4th, and 6th constraints are probabilistically active. The study in [35] identified the same active constraints plus the 7th constraint. Based on their reliability values, the three most critical constraints (with the highest p_f), are the 6th, 3rd, and 1st with failure probabilities of 0.003, 0.0017, and 0.0016, respectively. The same ranking was identified in [35] although the values of the component probabilities of failure were slightly different.

6. SUMMARY AND CONCLUSIONS

A simulation-based, system RBDO methodology has been presented using a trust-region approach and probabilistic re-analysis (PRRA). At each cycle of the trust-region approach, the PRRA estimates the system probability of failure p_{sys} at the current design, and the sensitivities of p_{sys} with respect to the design variables, using a single MC simulation. Both p_{sys} and its sensitivities are smooth in the design space because there is no numerical noise due to random sampling. This allows us to use efficient gradient-based optimizers. The developed RBDO method can handle problems with multiple disjoint failure regions and multiple most-probable points.

The overall methodology was demonstrated using a vibration absorber example with two disjoint failure domains, and a system RBDO of an internal combustion engine. The latter example demonstrated that the trust-region approach converges fast to the optimum design. Also, both examples demonstrated that the PRRA method calculates the system and component failure probabilities accurately, as verified by MC simulation.

Current and future research concentrates on the development of a metamodeling technique using importance sampling, a niching genetic algorithm, and a lazy learning method for local metamodeling. The technique provides "accuracy-on-demand" based on a user-specified, leave-one-out cross validation mean squared error. The metamodel will be used in the proposed RBDO method to further improve its computational efficiency.

REFERENCES

1. Kirsch, U., Bogomolni, M., and Sheinman, I., “Efficient Procedures for Repeated Calculations of the Structural Response Using Combined Approximations,” *Structural and Multidisciplinary Optimization*, 32, 435–446, 2006.
2. Rahman, S., and Xu, H., “A Univariate Dimension-Reduction Method for Multi-Dimensional Integration in Stochastic Mechanics,” *Probabilistic Engineering Mechanics*, 19, 393-408, 2004.
3. Youn, Byeng D., and Wang, P. F., “Complementary Interaction Method for System Reliability Analysis,” *2007 SAE World Congress*, Detroit, MI, Special Publication SP-2119, Paper 2007-01-0558, 143-153, 2007.
4. Kim, N.-H., and Ramu, P., “Tail Modeling in Reliability-Based Design Optimization for Highly Safe Structural Systems,” *47th AIAA/ASME/ASCE/AHS/ASC Structures, Structural Dynamics, and Materials Conference*, May 1-4, Newport, RI, AIAA 2006-1825, 2006.
5. Farizal, and Nikolaidis, E., “Assessment of Imprecise Reliability Using Efficient Probabilistic Reanalysis,” *2007 SAE World Congress*, Detroit, MI, Special Publication SP-2119, Paper 2007-01-0552, 71-88, 2007.
6. Zhang, G., Nikolaidis, E., and Mourelatos, Z. P., “An Efficient Re-Analysis Methodology for Probabilistic Vibration of Large-Scale Structures,” in press, *Journal of Mechanical Design*, 2009.
7. Rackwitz, R., and Fiessler, B., “Structural Reliability under Combined Random Load Sequences,” *Computers and Structures*, 9(5), 484-494, 1978.
8. Breitung, K., "Asymptotic Approximations for Multinormal Integrals," *ASCE Journal of Engineering Mechanics*, 110, 357-366, 1984.

9. Der Kiureghian, A., and T. Dakessian, “Multiple Design Points in First and Second-Order Reliability,” *Structural Safety*, 20(1), 37-49, 1998.

10. Bucher, C. G., “Adaptive Sampling – An Iterative Fast Mote Carlo Procedure,” *Structural Safety*, 5, 119-126, 1988.

11. Melchers, R. E., “Improved Importance Sampling Methods for Structural System Reliability Calculation,” *Proceedings of International Conference on Structural Safety and Reliability (ICOSSAR)*, 1185-1192, 1989.

12. Karamchandani, A., Bjerager, P., and Cornell, C. A., “Adaptive Importance Sampling,” *5th International Conference on Structural Safety and Reliability*, (Eds. Ang, A. H.-S., Shinozuka, M. and Schuëller, G. I.), ASCE, 855-862, New York, 1989.

13. Mahadevan, S., and Raghothamachar, P., “Adaptive Simulation for System Reliability Analysis of Large Structures,” *Computers and Structures*, 77, 725-734, 2000.

14. Zou, T., Mahadevan, S., Mourelatos, Z. P., and Meernik, P. R., “Reliability Analysis of Automotive Body-Door Subsystem,” *Reliability Engineering and System Safety*, 78(3), 315-324, 2002.

15. Cornell, C. A., “Bounds on the Reliability of Structural Systems”, *Journal of Structural Division*, 93 ST1, 171-200, 1967.

16. Ditlevsen, O., “Narrow Reliability Bounds for Structural Systems”, *Journal of Structural Mechanics*, 7(4), 453-472, 1979.

17. Schueller, G. I., and R. Stix., “A Critical Appraisal of Methods to Determine Failure Probabilities” *Structural Safety*, 4(4),293-309

18. Fu, G., and Moses, F., “Multimodal Simulation Method for System Reliability Analysis”, *Journal of Engineering Mechanics*, 119(6), 1173-1179, 1993.

19. Ditlevsen, O., and Bjerager, P., “Plastic Reliability Analysis by Directional Simulation”, *DCAMM Report*, 353, Technical University of Denmark, Lyngby, Denmark, June 1987.

20. Au, S. K., and Beck, J. L., “A New Adaptive Importance Sampling Scheme for Reliability Calculations,” *Structural Safety*, 21, 135-158, 1999.

21. Meeker, W. Q., and Escobar, L. A., *Statistical Methods for Reliability Data*, John Wiley & Sons, 1998.

22. Aldrich, J., "R. A. Fisher and the Making of Maximum Likelihood," *Statistical Science*, 12 (3), 162-176, 1997.

23. Harbitz, A., “An Efficient Sampling Method for Probability of Failure Calculation,” *Structural Safety*, 3, 109-115, 1986.

24. Grooteman, F., “Adaptive Radial-Based Importance Sampling Method for Structural Reliability,” *Structural Safety*, 30, 533-542, 2008.

25. Kuczera, R., Mourelatos, Z. P., and Latcha, M., “A Monte Carlo Reliability Assessment for Multiple Failure Region Problems using Approximate Metamodels,” *Proceedings of ASME Design Engineering Technical Conferences*, DETC2007-34957, 2007.

26. Shir, O. M., “Niching in Evolution Strategies,” *M.S. Thesis*, Leiden University, 2004.

27. Li, J., and Mourelatos, Z. P., “Reliability Estimation for Time-dependent Problems Using a Niching Genetic Algorithm”, *Proceedings of ASME Design Engineering Technical Conferences*, DETC2007-34865, 2007.

28. Aha, D. W., Editorial, Special Issue on Lazy Learning, *Artificial Intelligence Review*, 11(1-5), 1-6, 1997.

29. Birattari, M., Bontempi, G., and Bersini, H., "Lazy Learning Meets the Recursive Least-Squares Algorithm," *Advances in Neural Information Processing Systems 11*, Kearns, M. S., Solla, S. A., and Cohn, D. A., Eds., 375-381, MIT Press, Cambridge, MA, 1999.
30. Singh, A., Mourelatos, Z. P., and Li, J., "Design for Lifecycle Cost Using Time-Dependent Reliability", *Proceedings of ASME Design Engineering Technical Conferences*, DETC2009-86587, 2009.
31. Shan, S., and Wang, G. G., "Failure Surface Frontier for Reliability Assessment on Expensive Performance Function," *ASME Journal of Mechanical Design*, 128, 1227-1235, 2006.
32. Zou, T., Mourelatos, Z. P., Mahadevan, S., and Tu, J., "An Indicator Response Surface for Simulation-Based Reliability Analysis," *ASME Journal of Mechanical Design*, 130(7), 071401-1-11, 2008.
33. Papalambros, P. Y. and Wilde, D. J., *Principles of Optimal Design; Modeling and Computation*, 2nd Edition, Cambridge University Press, New York, 2000.
34. McAllister, C. D., and Simpson, T. W., "Multidisciplinary Robust Design Optimization of an Internal Combustion Engine," *ASME Journal of Mechanical Design*, 125(1), 124-130, 2003.
35. Liang, J., Mourelatos, Z. P., and Nikolaidis, E. (2007) "A Single-Loop Approach for System Reliability-Based Design Optimization," *ASME Journal of Mechanical Design*, 129, 1215-1224, 2007.